JOURNAL OF MATERIALS SCIENCE 27 (1992) 4791–4796

Sintering and compensation effect of donor- and acceptor-codoped 3 mol% Y_2O_3–ZrO_2

HONG-YANG LU
Institute of Materials Science and Engineering, National Sun Yat-Sen University, Kaohsiung 80424, Taiwan

SAN-YUAN CHEN*
Materials Research Laboratories, Industrial Technology Research Institute, Chutung 31015, Taiwan

Addition of ~0.15–0.5 mol% acceptor oxide, Al_2O_3, to 3 mol% Y_2O_3–ZrO_2 results in enhanced densification at 1350 °C. The enhancement is accounted for by a liquid phase sintering mechanism. The addition of donor oxide, Ta_2O_5, of 0.15–2.5 mol% at 1300–1600 °C results in the destabilization of tetragonal (t-) phase and the decrease of final density in 3 mol% Y_2O_3–TZP (tetragonal ZrO_2 polycrystals). X-ray diffractometry (XRD) reveals that the Ta_2O_5-added 3 mol% Y_2O_3–ZrO_2 contains monoclinic (m-) ZrO_2 and a second phase of $Ta_2Zr_6O_{17}$. The decreasing in final density is attributed to the increase of m-ZrO_2 content. Complete destabilization of t-ZrO_2 to m-ZrO_2 in samples added with 2.5 mol% Ta_2O_5 is interpreted by the compensation effect based on donor- and acceptor-codoping defect chemistry.

1. Introduction

Minor addition of Al_2O_3 was found to enhance the densification of Y_2O_3-stabilized ZrO_2 compositions [1–5]. A liquid phase sintering mechanism [2, 3] was proposed to account for the enhancement. This liquid containing Y_2O_3, Al_2O_3 and SiO_2 [6, 7] residued to grain boundaries after cooling to room temperature was responsible for densification improvement [3]. Nevertheless, at 1300 °C, the mass transport increased via a doping mechanism [2] due to the limited solid solution of ~ 0.1 mol% Al_2O_3 in ZrO_2 [5] has also been reported to assist the densification of the ceramic. Electrical conductivity measurement [2] supported this solid state doping of Al^{3+} to ZrO_2. Second phase pinning was also suggested [3] for the grain growth inhibition observed in the Al_2O_3-added Y_2O_3-FSZ (fully stabilized ZrO_2). Destabilization of the t-ZrO_2 in 3 mol% Y_2O_3–ZrO_2 compositions was attributed to the partition effect where Y_2O_3 was drawn from the tetragonal ZrO_2 grain to the liquid phase [7].

Taking the terminology of donor and acceptor as normally used in semiconductors, Ta^{5+} is a donor ion when it substitutes Zr^{4+} lattice site giving up one electron and forms a positively charged defect $Ta_{Zr}^{\cdot}$; and Al^{3+} is an acceptor ion when it substitutes Zr^{4+} lattice site accepting one electron and results in a negatively charged defect Al'_{Zr} [8]. The addition of Ta_2O_5 to Y_2O_3–ZrO_2 compositions, leading to the decrease of the critical grain size for the tetragonal (t) to monoclinic (m) phase transformation, was reported by Kim and Tien [9]. The transformability of t-ZrO_2 to m-ZrO_2 was [9] further related to the increase in the c/a ratio of Y_2O_3–TZP.

Donor and acceptor of compensating concentrations were found [10, 11] to restore the semiconductivity in donor-doped $BaTiO_3$ to the room temperature resistivity. The high temperature phases, cubic (c-) and t-ZrO_2 are retained to room temperature when ZrO_2 is doped with acceptor oxides, such as MgO and Y_2O_3. The retention of the high-temperature phase would be counteracted by the compensation effect. The compensation effect in ZrO_2 compositions can thus be investigated by further codoping the acceptor-doped (3 mol% Y_2O_3) ZrO_2 with either acceptor oxide, Al_2O_3, or with donor oxide, Ta_2O_5, respectively. This work describes the sintering behaviour, and possible mechanism of densification of these powder mixtures. The compensation effect due to the donor- and acceptor-codoping in these compositions is then explained.

2. Experimental procedure

3 mol% Y_2O_3–ZrO_2 powder (TZ3Y, Toyo Soda, Japan) containing trace impurities of 100 p.p.m. (wt) of SiO_2, 20 p.p.m. (wt) of Fe_2O_3 and 70 p.p.m. (wt) of

Present address: Department of Materials Science and Engineering, University of Michigan, Ann Arbor, Michigan, USA

Na_2O was used in this study. This powder was blended with appropriate quantities of 0.05–5.0 mol % Al_2O_3 powder (AKP-50, Sumitomo, Japan) and mixed in a high purity (> 99.9% pure) Al_2O_3 ball mill with 3 mol % Y_2O_3–ZrO_2 balls (Toyo Soda, Tokyo, Japan), using deionized water medium. It was followed by oven drying at 110 °C. Ta_2O_5 (reagent grade, Merck, FRG) of 0.15–5.0 mol % was added in the oxide form to TZ3Y powder and then followed by the same procedures of ball milling and drying. The dried powder was then deagglomerated by using an agate mortar and pestle before being dry-pressed to discs of 12 mm diameter in a WC-inserted steel die at a pressure of ~ 100 MPa. These discs were then sintered at temperatures of 1250–1600 °C for 2–12 h. Final density (ρ_F) was measured by Archimedes' method using deionized water as dispersing media. Relative final density (ρ_{rel}) was calculated by:

$$\rho_{rel} = (\rho_F/\rho_{TD}) \times 100\%$$

where the theoretical density of tetragonal ZrO_2, $\rho_{TD} = 6100\ kg\,m^{-3}$ [12]. Sintered samples were then mechanically ground to ~ 30 μm before being lapped from 12 μm to 1 μm surface roughness successively with diamond paste. For transmission electron microscopy (TEM), these lapped samples were then dimpled before being Ar^+-ion thinned to electron transparency. Scanning electron microscopy (SEM) coupled with energy dispersive spectroscopy (EDX) analysis and TEM were used for microstructural analysis. Grain size was determined by the linear intercept method as described by Mendelson [13]. Crystalline phases were identified by a Philips PW1820 diffractometer with a CuK_α radiation operating at 40 kV, 30 mA. Phase content of ZrO_2 was determined by XRD followed the technique developed by Garvie and Nicholson [14].

3. Results

3.1 Effect of Al_2O_3 addition

3.1.1 General

A relative final density (ρ_{rel}) of ~ 99.7% TD (theoretical density) was obtained when 0.15–0.5 mol % Al_2O_3-added TZ3Y powder was sintered at 1350–1400 °C for 2 h (Fig. 1a). When the sintering temperature was raised to 1600 °C, for the same range of dopant concentration, however, lower final densities (Fig. 1b) of ~ 95.7–96.0% TD were obtained. An optimal final density for 0.15–5.0 mol % Al_2O_3 addition occurred at ~ 1350 °C (Fig. 1a). Sintering at 1500 °C and 1600 °C resulted not only in lower final densities, but also a completely different dependence of ρ_{rel} on Al_2O_3 concentration (compare Fig. 1a with Fig. 1b). As the dopant level increased, the relative final density decreased before increasing again at high Al_2O_3 concentration (Fig. 1b). And the maximum final density was obtained at ~ 0.15 mol % Al_2O_3 addition for samples sintered at 1500 °C and 1600 °C.

The m-ZrO_2 phase content increased progressively from less than 10% of the 0.5 mol % Al_2O_3-added samples sintered at 1300 °C for 2h to ~ 45% when the sintering temperature was raised to 1600 °C for 2h

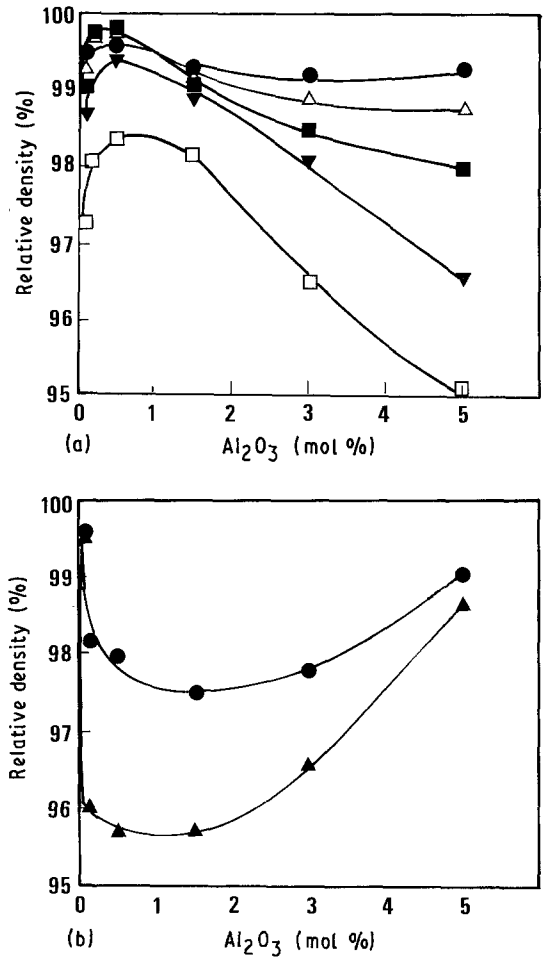

Figure 1 (a) Relative final density of Al_2O_3-added 3 mol % Y_2O_3–ZrO_2 when sintered at 1200–1450 °C for 2 h. (●) 1450 °C, (△) 1400 °C, (■) 1350 °C, (▼) 1300 °C, (□) 1250 °C. (b) Relative final density of Al_2O_3-added 3 mol % Y_2O_3–ZrO_2 when sintered at 1500–1600 °C for 2 h. (●) 1500 °C, (▲) 1600 °C.

(Fig. 2). For the unadded TZ3Y samples, the m-ZrO_2 content was barely detectable when sintered for less than 5 h. The amount of m-ZrO_2 in these unadded samples remained < 45% even with prolonged heating for 9 h at 1600 °C. For 0.5 mol % Al_2O_3 addition, however, m-ZrO_2 phase content was found to increase with both sintering temperature and time (Fig. 2). If the critical grain size for t–m phase transformation is taken as the average grain size of the sample containing 5% m-ZrO_2 phase (5% is approximately the detection limit of XRD), this critical grain size (G_{crit}) decreased from 1.30 μm [9] of the unadded to 0.6 μm of the TZ3Y samples added with 0.5 mol % Al_2O_3.

3.1.2 Densification

Densification enhancement by adding Al_2O_3 was greatest when 0.5 mol % Al_2O_3 (Fig. 3) was sintered at 1350 °C for less than 15 min. A significant improvement of the relative final density of ~ 90% TD obtained within 10 min of sintering was only better than the ~ 80% TD of unadded samples. The enhancement was comparatively less significant when samples were sintered at the higher temperature of 1600 °C. The densification rate of a ceramic powder compact is taken as the first derivative of the densification curve described by plotting the relative final

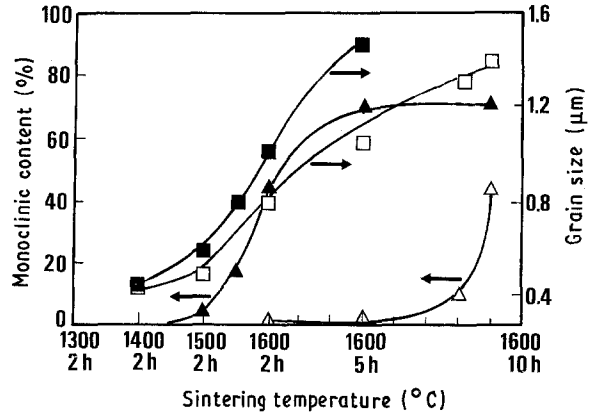

Figure 2 Increase of m-ZrO_2 content and average grain size for the 0.5 mol % Al_2O_3-added TZ3Y powder (▲, ■) when sintered at 1200–1600 °C. (△, □) TZ3Y.

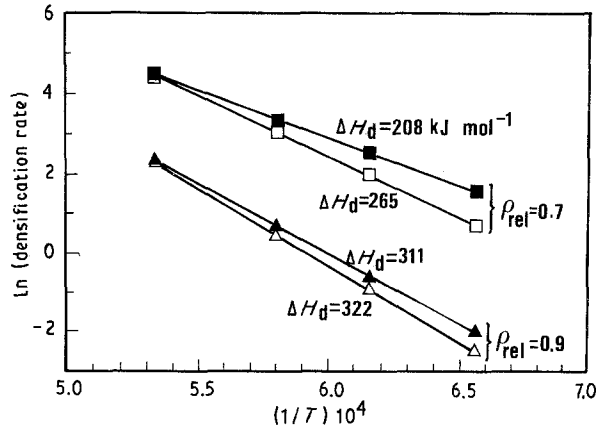

Figure 4 Activation enthalpy derived from the densification curves in Fig. 3.

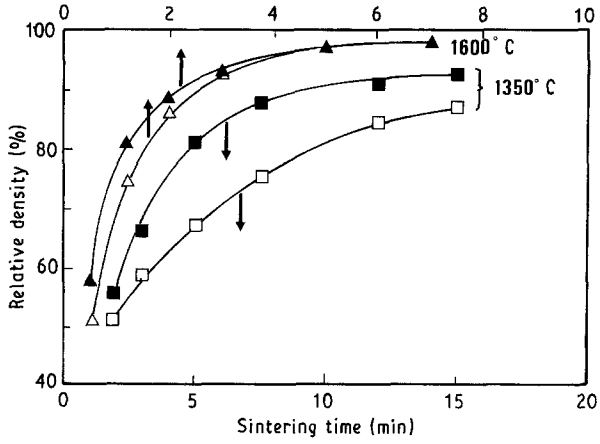

Figure 3 Densification curves for the 0.5 mol % Al_2O_3-added (▲, ■) and the unadded (△, □) 3 mol % Y_2O_3–ZrO_2 sintered at 1350 °C and 1600 °C.

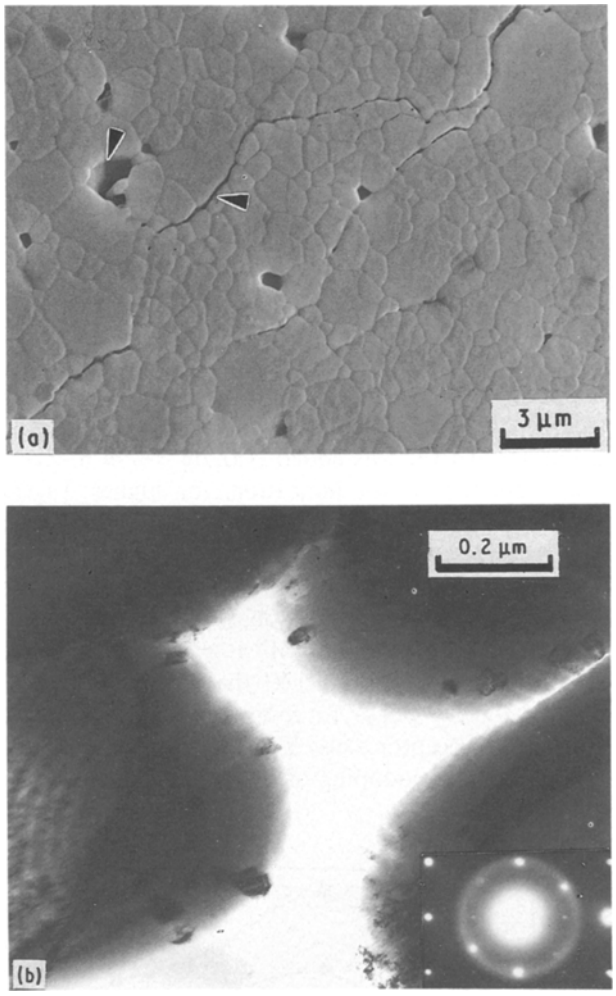

Figure 5 (a) Residual pores and intergranular cracks in 0.5 mol % Al_2O_3-added TZ3Y samples sintered at 1600 °C for 10 h. (b) Glassy grain boundary phase in Al_2O_3-added TZ3Y samples revealed by TEM.

density against sintering time. The densification rate at a particular relative final density was then obtained by drawing the tangent to the densification curve at the corresponding relative final density (ρ_{rel}), e.g. $\rho_{rel} = 0.6$, 0.7 and 0.9 of theoretical density as shown in Fig. 4. The densification curves for 0.5 mol % Al_2O_3-added TZ3Y is given in Fig. 3 for sintering at 1350 °C and 1600 °C respectively. The activation enthalpy for densification (ΔH_d) was then obtained by plotting the logarithm of densification rate ($\ln(d\rho/dt)$) against the reciprocal temperature ($1/T$ in K^{-1}), as shown in Fig. 4. ΔH_d values for densification in the later stages of sintering ($\rho_{rel} = 0.9$) are higher than those of the intermediate stage ($\rho_{rel} = 0.7$).

3.1.3 Microstructural features

The unadded TZ3Y powder after sintering yielded a homogeneous microstructure of average grain size of ~ 1 μm, which is similar to that observed in previous studies [15, 16]. Addition of Al_2O_3 gave a typical liquid phase sintered microstructure with rounded grains of bimodal grain size distribution (Fig. 5a), which was also similar to the MgO-added TZ3Y composition [16]. Residual pores and intergranular cracks were characteristic features observed in the Al_2O_3-added samples (as indicated in Fig. 5a). For those with 0.5 mol % Al_2O_3 addition and sintered at 1600 °C for 5 h, large grains exhibited the typical t + c "tweed" contrast [17] under TEM. These large grains had grown at the expense of the surrounding small grains by a coalescence mechanism [16]. TEM observations also revealed a grain-boundary phase of glassy

nature as seen in BFI (bright field image) (Fig. 5b), and indicated by a diffused halo in selected area diffraction (SAD) pattern.

3.2 Effect of Ta_2O_5 addition

3.2.1 General

There was no significant decrease in the final relative density of sintered TZ3Y powder compacts from a small Ta_2O_5 addition of 0.15 mol % and 1.0 mol % when sintered at 1300 °C and 1400 °C for 2 h. For higher sintering temperatures, i.e. 1500 °C and 1600 °C (Fig. 6), the relative final density decreased with higher sintering temperature, and also with higher Ta_2O_5 concentration. This trend was most pronounced with 1.0 mol % addition. The maximum density of ~ 99.0% TD obtained by adding donor oxide Ta_2O_5, occurred at 1.0 mol % for 1400 °C sintering. Yet, the unadded TZ3Y powder was better sintered to a final density of ~ 99.6% at 1500 °C for 2 h. When the addition of Ta_2O_5 reached 2.5 mol %, regardless of the sintering temperature, final densities were generally lower (Fig. 6) than those of the samples studied in this category. A decrease of relative final density from ~ 99.5% to ~ 92.0% was seen with 2.5 mol % Ta_2O_5 addition when sintered at 1600 °C for 2 h.

3.2.2 The t–m phase transformation

The m-ZrO_2 phase content increased with sintering temperature and with the level of Ta_2O_5 addition (Fig. 7) when sintered for 2 h except when the 2.5 mol % Ta_2O_5 was added. Taking 5% of m-ZrO_2 phase content as an indication, for higher Ta_2O_5 additions, m-ZrO_2 started to emerge at lower sintering temperatures; i.e. 1.5 mol %/1300 °C versus 0.15 mol % /1500 °C (Fig. 7). The sintered compacts contained ~ 100% m-ZrO_2 phase when Ta_2O_5 addition reached 2.5 mol % for all sintering temperatures studied (Fig. 7). This indicates that metastable retention of t-ZrO_2 phase to room temperature by the addition of acceptor oxide Y_2O_3 has been completely reverted by the codoping of Ta_2O_5 donor oxide.

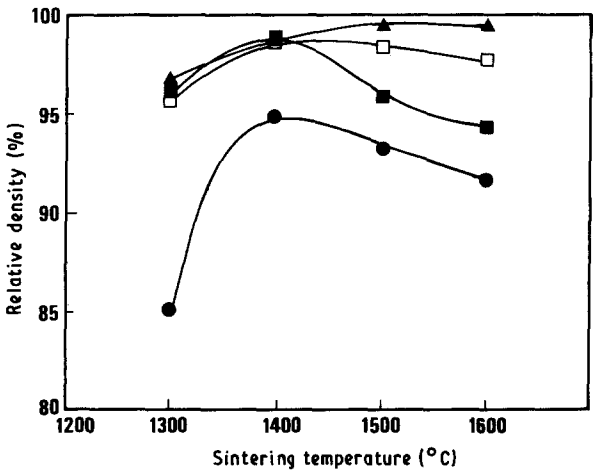

Figure 6 Relative final density of Ta_2O_5-added 3 mol % Y_2O_3–ZrO_2 (xTa_2O_5–$(1-x)$TZ3Y) when sintered at 1300–1600 °C for 2 h. (▲) $x = 0$, (□) $x = 0.0015$, (■) $x = 0.01$, (●) $x = 0.025$.

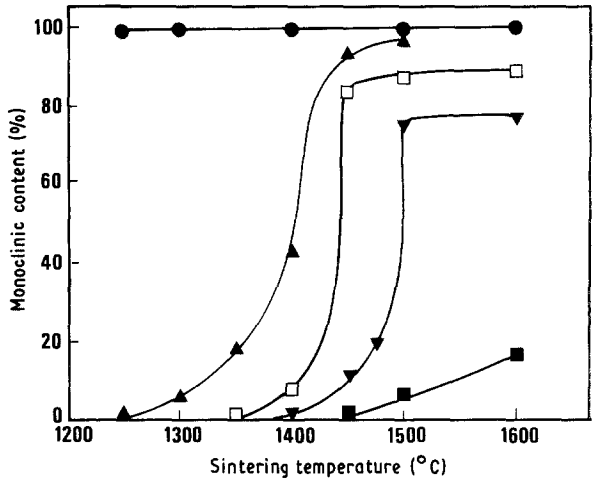

Figure 7 Increase of m-ZrO_2 content with Ta_2O_5 addition and sintering temperature. x Ta_2O_5–$(1-x)$TZ3Y: (■) $x = 0.0015$, (▼) $x = 0.005$, (□) $x = 0.01$, (▲) $x = 0.015$, (●) $x = 0.025$.

The critical grain size for the t–m phase transformation dropped sharply from 1.30 μm to 0.55 μm with only a small addition of 0.15 mol % Ta_2O_5. Further addition of Ta_2O_5 resulted in a critical grain size of ~ 0.45 μm (Fig. 8) for the t–m phase transformation.

3.2.3 Microstructural features

Ta_2O_5-added samples sintered at 1500 °C for 2 h, having dispersed pores and an average grain size of ~ 1 μm, were poorly densified (Fig. 9a). Cracks were also found when the Ta_2O_5 addition was less than 2.5 mol % (Fig. 9a). When the Ta_2O_5 codoping level was increased to 5.0 mol %, a typical microstructure comprised larger ZrO_2 grains with dispersed second phases located either intergranularly or in triple junctions (Fig. 9b). Grains exhibiting surface upheaval, as indicated in SEM micrograph (Fig. 9b), are characteristic of the transformed m-ZrO_2 phase [18]. Intergranular cracks were found adjacent to the transformed ZrO_2 grains consistent with the volume

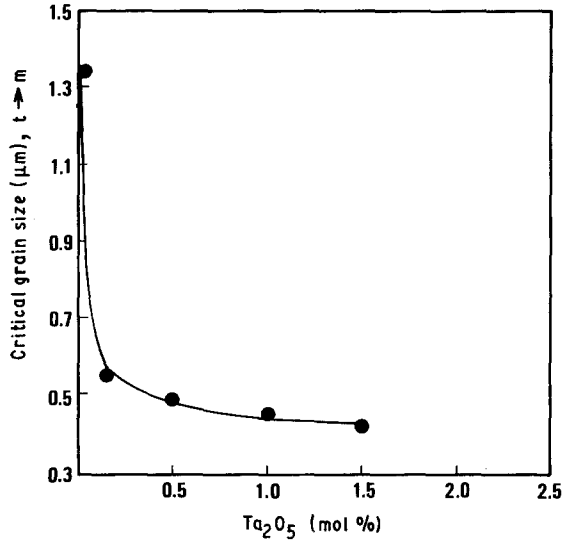

Figure 8 Critical grain size for t–m phase transformation when Ta_2O_5 added to 3 mol % Y_2O_3–ZrO_2.

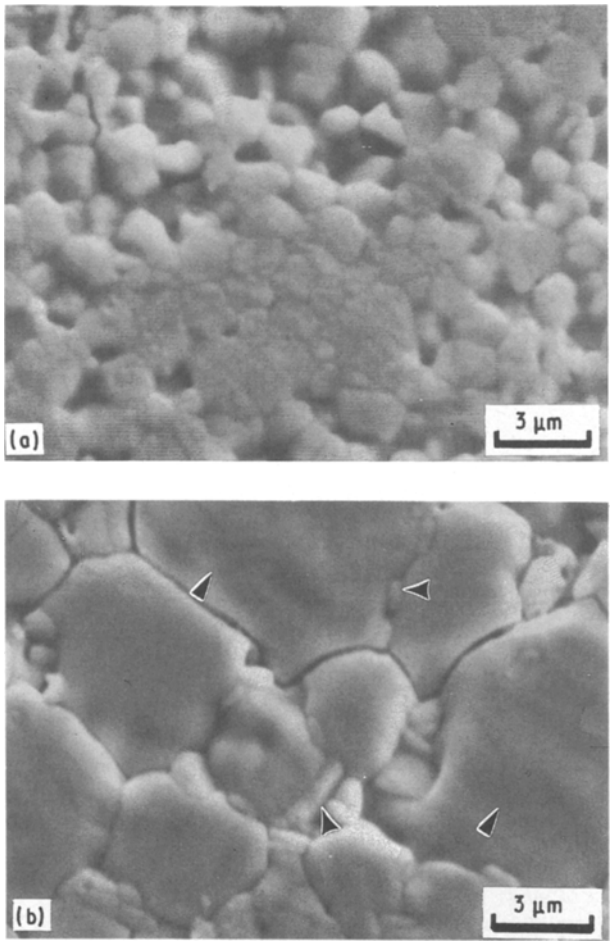

Figure 9 Sintered samples with Ta_2O_5 addition, surface upheaval and second phase were observed in (b) (SEM).

expansion accompanying the transformation [19]. This second phase was identified by XRD as $Ta_2Zr_6O_{17}$.

4. Discussion

4.1 Liquid phase sintering

Trace impurities, such as SiO_2 associated with the starting TZ3Y powder, react with Al_2O_3 additive to form a ternary Y_2O_3–Al_2O_3–SiO_2 eutectic liquid at sintering temperatures. Densification enhancement by a small addition of Al_2O_3 can be attributed to liquid formation at sintering temperatures, as previously proposed [1–3]. An extensive solid solution exists between Ta_2O_5 and the trace impurity SiO_2, however, which would not allow the liquid to form at sintering temperatures unless the temperature exceeded the lowest binary eutectic of the Ta_2O_5–SiO_2 system at $\sim 1570\,^{\circ}C$ [20]. The liquid phase is therefore expected to play a minor role in the sintering of Ta_2O_5-added TZ3Y powder at temperatures $< 1570\,^{\circ}C$.

The activation enthalpy, ΔH_d, describes the combination of matter transport processes concurrent during liquid phase sintering [21]. Lower ΔH_d value (265 versus 208 kJ mol^{-1}) indicates a liquid-assisted densification due to minor Al_2O_3 addition of 0.5 mol % (Fig. 4). This improved densification is particularly apparent during the intermediate stage of sintering, where $\rho_{rel} = 70\%$ TD. As densification proceeds to $\rho_{rel} \sim 90\%$ TD, the controlling mechanism could have been solid state diffusion [2]. Since the sintering mechanism is predominantly solid state for the unadded powder, that results in similar ΔH_d values (311 versus 322 kJ mol^{-1}) for the unadded and the Al_2O_3-added TZ3Y powder.

4.2 Defect chemistry and densification by solid state

The addition of 0.15–0.5 mol % Al_2O_3 resulted in improving the densification at 1350 °C (Fig. 1a) and in reducing the final sintered density at 1600 °C (Fig. 1b). The hindrance described by the decrease in relative final density was most pronounced at the addition levels of 0.15 and 0.5 mol % (Fig. 1b), where for 0.5 mol % Al_2O_3 addition, the m-ZrO_2 phase content was approximately $\sim 45\%$ (Fig. 2). This indicates that in fact densification at 1600 °C was not hampered and was still assisted by the liquid phase, as was the sintering at 1350 °C. The transformation of t-ZrO_2 to m-ZrO_2 (of lower theoretical density, $\rho_{TD} = 5560\,kg\,m^{-3}$ [12]) in an appreciable degree ($\sim 45\%$) resulted in the decrease in final density.

Y_2O_3, being an acceptor oxide for ZrO_2, stabilizes the high temperature cubic (c) and tetragonal (t) phases when added to ZrO_2. Here the oxygen vacancy ($V_O^{\cdot\cdot}$) created by adding stabilizing oxides, e.g. MgO, Y_2O_3 alike, was suggested [22] to play an important role in the stabilization. Al_2O_3 as well as Y_2O_3 is an acceptor oxide to ZrO_2. At 1300 °C, its dissolution of ~ 0.1 mol % [5] to c-ZrO_2 lattices occupies the Zr^{4+}-site and forms a substitutional defect, Al'_{Zr}. Supposing the intrinsic defect is the Schottky type and $V_O^{\cdot\cdot}$ is the principal charge compensating defect, we have the defect reaction equation:

$$Al_2O_3 \rightarrow 2\,Al'_{Zr} + V_O^{\cdot\cdot} + 3\,O_O^{\times}$$

The zirconium ion (Zr^{4+}), which diffuses through Zr-interstitials ($Zr_i^{\cdot\cdot\cdot\cdot}$), was proposed [23] to be the rate-controlling species and step for densifying acceptor-doped ZrO_2. The $V_O^{\cdot\cdot}$ formation will supplement the already existing oxygen vacancy by acceptor Y_2O_3. The formation of $V_O^{\cdot\cdot}$ would not significantly affect the densification by solid state to the reverse direction, since the $V_O^{\cdot\cdot}$ of ~ 0.1 mol % created by Al_2O_3 amounts to only $\sim 3\%$ of the $V_O^{\cdot\cdot}$ (3 mol %) by Y_2O_3. And, its effect of ~ 0.1 mol % on hindering the densification was overwhelmed by the liquid-phase-assisted densification. Following the same argument, when added with Ta_2O_5 donor, it is expected that without forming an appreciable amount of liquid phase, densification could not be enhanced significantly. And since the amount of m-ZrO_2 phase content increased at all levels of Ta_2O_5 addition (Fig. 7), then the drop in relative final density (Fig. 6) is accounted for by the lower theoretical density of m-ZrO_2.

4.3 Compensation effect

Grain growth inhibition resulting from MgO addition to Al_2O_3 ceramic could be counteracted by codoping with ZrO_2 of equimolar quantity [24]. The counteraction of semiconductivity created by adding a donor-dopant, such as La^{3+}, was owing to the compensation

effect previously proposed for the donor- and acceptor-codoped semiconducting $BaTiO_3$ [21, 22]. The room temperature resistivity was restored [21, 22] to the donor-doped $BaTiO_3$ by adding half the molar quantity of the acceptor oxide. For the donor- and acceptor-codoped ZrO_2, the neutrality approximation [8] can be written as follows:

$$[Ta_{Zr}^{\cdot}] + 2[V_O^{\cdot\cdot}] = [Y_{Zr}'] + 4[V_{Zr}''''] \quad (1)$$

This neutrality approximation predicts that the defect concentration due to acceptor substitution, $[Y_{Zr}']$, increases with that created by the donor, $[Ta_{Zr}^{\cdot}]$, by a slope of unity, i.e. in a direct proportional relationship. Both the decreasing of the critical grain size (from 1.30 μm to 0.55 μm to 0.45 μm) for the t–m transformation and the emerging of m-ZrO_2 with Ta_2O_5 addition (Figs 7 and 8) indicates that Ta_2O_5 donor-codoping leads to the destabilization of t-ZrO_2. And when the Ta_2O_5 concentration was increased to 2.5 mol %, the TZP of initially 100% tetragonal phase was transformed to 100% m-ZrO_2 (Fig. 7). Stabilization of t-ZrO_2 phase to room temperature is obtained by adding acceptor-dopant Y_2O_3 of 3 mol %. And the retention will be reverted when adding an equal amount of the counter-dopant, the donor Ta_2O_5 to the acceptor-doped ZrO_2. That is to say, the neutrality relationship is maintained as long as

$$[Ta_{Zr}^{\cdot}] - [Y_{Zr}'] = 0 \quad (2)$$

where acceptor and donor are compensated completely. Therefore, when an equal molar quantity of Ta_2O_5 is codoped, the stabilization of t-ZrO_2 phase by Y_2O_3 addition, is counteracted. It is expected from the neutrality approximation that t-ZrO_2 is destabilized and ZrO_2 is completely restored to its room temperature phase, the monoclinic. In fact, the molar quantities for donor and acceptor oxide were approximately equal in the present study, i.e. 2.5 mol % and 3 mol %. This would suggest that the stabilization of t-ZrO_2 by Y_2O_3 has actually been compensated for by codoping with Ta_2O_5.

Defect compensation as a controlling factor of abnormal grain growth in $BaTiO_3$ was reported by Brook *et al.* [25]. In the case of defect species $Ta_{Ti}^{\cdot}$ and Co_{Ti}'' formed in donor–acceptor codoped $BaTiO_3$, grain growth occurred when donor and acceptor were present in compensating concentrations. For our study, defect species of $Ta_{Zr}^{\cdot}$ and Y_{Zr}', present at equal molar quantities, are expected to compensate each other and to lead to grain growth.

5. Conslusions

1. Addition of Al_2O_3 acceptor oxide to 3 mol % Y_2O_3–ZrO_2 powder enhanced its densification by a liquid-assisted sintering mechanism.
2. Addition of Ta_2O_5 donor oxide to 3 mol % Y_2O_3–ZrO_2 powder destabilized the tetragonal ZrO_2 and resulted in lower final sintered densities.
3. Complete transformation of t-ZrO_2 to m-ZrO_2 with 2.5 mol % Ta_2O_5 addition to 3 mol % Y_2O_3–ZrO_2 was explained by a compensation effect.

Acknowledgements

Thanks are due to Dr Pouyan Shen for critical comments. Funding support by the Ministry of Economic Affairs of Taiwan through contract no. ITRI-047-P301(76) to the Industrial Technology Research Institute is gratefully acknowledged.

References

1. K. C. RADFORD, *J. Mater. Sci.* **14** (1979) 59–65.
2. R. C. BUCHANAN and D. M. WILSON, in "Advances in ceramics", vol. 10, Structure and properties of MgO and Al_2O_3, edited by W. D. Kingrey (The American Ceramic Society, Columbus, OH, 1984) p. 526.
3. E. P. BUTLER and J. DRENNAN, *J. Amer. Ceram. Soc.* **65** (1982) 474–478.
4. W. D. TOUHIG and T. Y. TIEN, *ibid.* **63** (1980) 595–596.
5. H. BERNARD, Microstructure of Y_2O_3-stabilised ZrO_2, PhD thesis, University of Grenoble, France (1981).
6. M. RUHLE, A. H. HEUER and N. CLAUSSEN (eds), in "Advances in ceramics", vol. 12, Science and technology of zirconia II (The American Ceramic Society, Columbus, OH, 1984) p. 352.
7. H. TSUBAKINO, R. NOZATO and M. HAMAMOTO, *J. Amer. Ceram. Soc.* **74** (1991) 440–443.
8. A. KROGER, "The chemistry of imperfect crystals", vol. 2 (North-Holland, Amsterdam, 1974).
9. D. J. KIM and T. Y. TIEN, in The American Ceramic Society 89th Annual Meeting, 126-B-87, 1987.
10. C. J. PENG and H. Y. LU, *J. Amer. Ceram. Soc.* **71** (1988) C-44–C-46.
11. C. J. TING, C. J. PENG, H. Y. LU and S. T. WU, *ibid.* **73** (1990) 329–334.
12. R. STEVENS, "Introduction to zirconia" (MEL Publications no. 113, Magnesium Elektron Ltd, London, UK, 1986).
13. M. I. MEDELSON, *J. Amer. Ceram. Soc.* **55** (1972) 303–305.
14. R. C. GARVIE and P. S. NICHOLSON, *ibid.* **55** (1969) 443–446.
15. H. Y. LU and S. Y. CHEN, *ibid.* **70** (1987) 537–541.
16. H. Y. LU and J. S. BOW, *ibid.* **72** (1989) 228–231.
17. R. H. J. HANNINK, *J. Mater. Sci.* **13** (1978) 2487–2496.
18. G. K. BANSAL and A. H. HEUER, *Acta Metall.* **20** (1972) 1281–1289.
19. Y. FU, A. G. EVANS and W. M. KRIVEN, *J. Amer. Ceram. Soc.* **67** (1984) 626–630.
20. Phase Diagrams for Ceramists, Figs 4447 and 4448 (The American Ceramic Society, Columbus, OH, 1975).
21. R. RAJ and C. K. CHYUNG, *Acta Metall.* **29** (1981) 159–166.
22. M. MORINAGA, H. ADACHI and M. TSUKUDA, *J. Phys. Chem. Solids* **44** (1983) 301–306.
23. S. WU and R. J. BROOK, *Solid State Ionics* **14** (1984) 123–130.
24. S. J. BENNISON and M. P. HARMER, *J. Amer. Ceram. Soc.* **69** (1985) C-22–C-24.
25. R. J. BROOK, in "Ceramic transactions–ceramic powder science", edited by G. L. Messing, E. R. Fuller and H. Hauser (The American Ceramic Society, Columbus, OH, 1988) p. 811.

Received 8 May
and accepted 12 September 1991